Yahya R. Hathal ¹ Isam M. Ibrahim ¹ Mohammed K. Khalaf ²

Department of Physics, College of Science, University of Baghdad, Baghdad, IRAQ
Department of Materials Research, Ministry of Science and Technology, Baghdad, IRAQ



Effect of Substrate Temperature on Characteristics and Gas Sensing Properties of Nb₂O₅/Si Thin Films

Thin films of Nb_2O_5 have been successfully deposited using the DC reactive magnetron sputtering technique to manufacture NH_3 gas sensors. These films have been annealed at a high temperature of 800°C for one hour. The assessment of the Nb_2O_5 thin films structural, morphological, and electrical characteristics was carried out using several methods such as X-ray diffraction (XRD), atomic force microscopy (AFM), energy-dispersive X-ray spectroscopy (EDS), Hall effect measurements, and sensitivity assessments. The XRD analysis confirms the polycrystalline composition of the Nb_2O_5 thin films with a hexagonal crystal structure. Furthermore, the sensitivity, response time, and recovery time of the gas sensor were evaluated for the Nb_2O_5 thin films at different operational temperatures. We have found that the NH_3 sensor has its highest sensitivity of 33.3% when manufactured with a power setting of 50 W at room substrate temperature (RT) and an operating temperature of 200°C . It also has a rapid response time of 10 seconds when utilizing a substrate temperature of 150°C . Additionally, the sample prepared with a substrate temperature of 100°C has the quickest recovery time, recorded at 30 seconds.

Keywords: Nb₂O₅ thin film; Sputtering; Substrate temperatures; Gas sensors Received: 04 November; Revised: 05 December; Accepted: 12 December 2023

1. Introduction

Niobium oxides are semiconductors that possess photocatalysis, functions such as electrochromic devices, and gas sensing. There are three stable forms of the combination of niobium with oxygen, namely NbO, NbO₂, and Nb₂O₅. Out of these materials, Nb₂O₅ exhibits the lowest Gibbs free energy of formation, making it the most thermodynamically favored for its formation [1]. Due to its desirable characteristics such as high refractive index, thermal stability, corrosion resistance, and a wide band gap, niobium oxide (Nb₂O₅) has been extensively studied as a promising material for gas sensors, catalysts, optical coatings, dye-sensitized solar cells, and displays. As an n-type transition material, Nb₂O₅ has gained significant attention in various research fields [2-4].

NH₃, a highly toxic chemical compound, poses significant risks to both humans and animals due to its ability to severely impede the body's oxygen consumption. Consequently, there is a pressing need to develop advanced materials that can effectively capture and detect NH₃ efficiently, ensuring the safety and well-being of individuals and living organisms [5].

Several methods have been employed to deposited thin films of Nb₂O₅, various thin film deposition techniques are available, including sputtering, ion beam sputtering (IBS), evaporation, oxidation, plasmaenhanced chemical vapor deposition (PECVD), spray pyrolysis, sol-gel, and pulsed-laser deposition (PLD) [6-10]. Sputtering is favored for its high deposition rates, uniform films, consistent composition, and strong adhesion. It yields dependable outcomes and enables the uniform application of thin films with consistent thickness over expansive substrates. Additionally, commercially accessible sputtering

systems facilitate the deposition of thin films that exhibit a remarkable balance between transparency and conductivity [11,12]. The primary objective of this study is to produce Nb_2O_5 thin films using dc magnetron sputtering for the purpose of creating NH_3 gas sensors based on Nb_2O_5/Si structures. A comprehensive examination has been carried out to investigate the influence of sputtering power on the structural, morphological, optical features, and sensing capabilities of these thin films.

2. Experimental Part

Niobium oxide thin films were expertly prepared on silicon wafers and quartz substrates using a highly effective dc reactive magnetron sputtering method. There are two main reasons to use magnetron, first reason is increasing the plasma density near the target's surface, second reason preventing secondary electrons from contributing to increased substrate temperature and radiation damage. A robust dc power of 50 W was consistently maintained throughout the process, producing exceptional thin films with superior properties. This deposition process was conducted at three distinct substrate temperatures: room temperature (RT), 100°C, and 150°C. The primary aim was to scrutinize the impact of these varied substrate temperatures on the structural characteristics and surface topography of the niobium oxide thin films.

Figure (1) shows the experimental setup for the dc sputtering system. The setup includes a glass vacuum chamber measuring 30 cm in diameter and 25 cm in height. Inside the chamber is a cathode in the form of a niobium target supplied by Aldrich, which has a high degree of purity (~99.99%). The target is circular, measuring 5 cm in diameter and 3 mm in thickness. It

is positioned 5 cm away from the anode. The niobium target is connected to a variable high-voltage dc power source. Magnetrons can be classified as either balanced or unbalanced, depending on the configuration of the magnets. In a balanced magnetron, all magnetic field lines are closed loops. In an unbalanced magnetron, some magnetic field lines are open and directed towards the chamber walls (type 1) or towards the substrate (type 2). Figure (2) shows a schematic representation of the possible magnet configurations, and in our research, we used planar magnetron sputtering (the closed-field unbalanced magnetrons configuration sputtering).

In preparation for film deposition, thoroughly cleaning the quartz substrates was carried out using an ultrasonic bath with isopropanol and deionized water, followed by nitrogen gas. Sputtering was executed using high-purity argon as the sputtering gas and oxygen as the reactive gas. The chamber underwent evacuation to reach a base pressure of 4.2x10⁻² mbar through a diffusion pump. During sputtering, a mass flow controller introduced oxygen and argon gases into the vacuum chamber, maintaining a constant argon flow rate of 50 sccm and 5 sccm for oxygen. The working and reactive gases were premixed in a small chamber before being introduced into the vacuum chamber. Deposition lasted for 120 minutes, followed by annealing of the films in ambient air at 800°C for one hour. The thickness of the prepared film at a sputtering power of 50 W and room temperature (RT) was 543 nm.

Gas sensor testing system is a customized setup with a stainless-steel test chamber that has gas inlets, an air admittance valve, and a multi-pin feedthrough for electrical connections. The sensor's temperature is regulated with a heater, and measurements are taken using a PC-interfaced digital multimeter and laptop. Gas flow is regulated using needle valves, which allows testing at air mixing ratios of NH₃ at 31.82 ppm. The experimental investigation covers a temperature range of 30 to 250 °C.

A Shimadzu XRD-6000 X-ray diffractometer was used to analyze the crystalline structure of the sample. The analysis was performed using CuK_{α} radiation with a wavelength of 0.154 nm, covering a 2θ range of 10° to 90°. Statistical and image analyses were carried out using ImageJ and OriginLAB software. A Vega Tescan TS 5130-LSH instrument was used for quantitative elemental analysis by Energy-dispersive x-ray spectroscopy (EDS). A Shimadzu UV-1650 PC UV-VIS spectrophotometer was used to determine the optical absorption spectra and then the optical energy bandgap of the deposited thin films, which spanned from 300 to 1100 nanometers. The van der Pauw method with the Ecopia HMS-3000 Hall Measurement was used to conduct Hall measurements. An Angstrom Advanced AA3000 atomic force microscope (AFM) was used to assess surface roughness and grain size distribution. Sensing measurements were carried out using a customdesigned system.

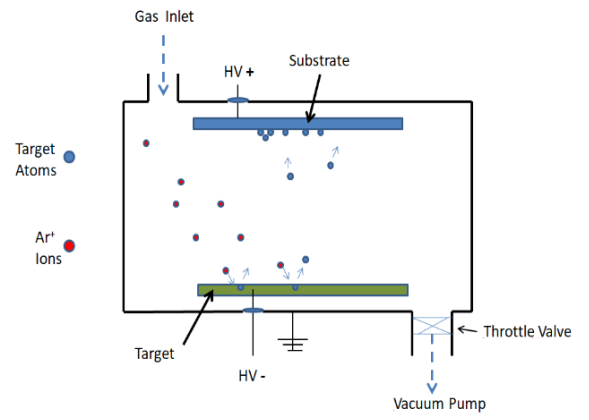


Fig. (1) A schematic representation of a dc sputtering system

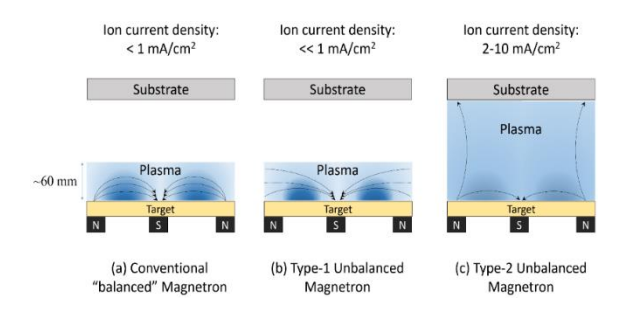


Fig. (2) A schematic representation of (a) conventional and (b) type-1 and (c) type-2 unbalanced magnetron sputtering systems $\frac{1}{2}$

3. Results and Discussion

The x-ray diffraction (XRD) patterns of the Nb₂O₅ thin film samples prepared with a constant dc power of 50W onto quartz substrates at different temperatures (RT, 100°C, and 150°C) are presented in Fig. (3). Hexagonal polycrystalline Nb₂O₅ structure was observed in all the samples. This was evident from the presence of four distinct peaks corresponding to the (001), (100), (101), and (002) lattice planes, which were observed at $2\theta = 22.3834^{\circ}$, 28.5233° , 36.7617° , and 46.1140°, respectively [13]. The observed peaks were found to match JCPDS card no. 00-028-0317 [14]. Elevating the substrate temperature resulted in a significant improvement in the crystallinity of the samples [15]. Moreover, increasing the substrate temperature leads to narrower diffraction lines, indicating a larger crystallite size. This phenomenon can be attributed to the energy provided by the higher temperature, which allows the atoms to be more arrangement during the thin film growth. Additionally, the thermally activated process of grain boundary migration and coalescence plays a role in this phenomenon. As the substrate temperature increases, the kinetic energy of the atoms increases, leading to the movement and merging of smaller crystallites. In our results, we noticed that increasing the crystallinity causes a decrease in crystal defects and dislocations, as well as the lattice strain produced by the nano-size effect [16].

The crystallite size (C.S) corresponding to the observed peaks were quantified and are outlined in Table (1). Furthermore, table (1) encompasses data regarding the positions of the peaks, their respective Miller indices for the diffraction planes, and the corresponding values for Full-Width at Half Maximum (FWHM).

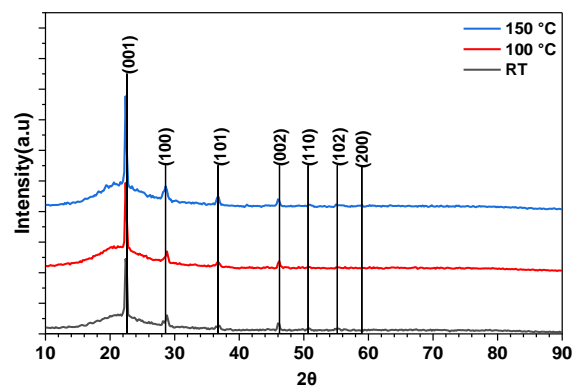


Fig. (3) XRD patterns for $Nb_2O_5\, thin$ films deposited at different substrate temperatures

Table (1) XRD parameters for Nb_2O_5 thin films deposited at different substrate temperatures

TS (°C)	2θ (deg.)	FWHM (deg.)	d _{hki} Exp. (Å)	C.S (nm)	d _{hk} l Std. (Å)	hkl
	22.4312	0.3727	3.9604	21.7	3.9300	(001)
RT	28.8199	0.4259	3.0953	19.3	3.1200	(100)
	36.8057	0.6110	2.4400	13.7	2.4460	(101)
	46.0958	0.4259	1.9676	20.3	1.9620	(002)
	22.3834	0.3368	3.9687	24.0	3.9300	(001)
100	28.8083	0.4182	3.0966	19.6	3.1200	(100)
	36.7358	0.4922	2.4445	17.0	2.4460	(101)
	46.1917	0.4145	1.9637	20.8	1.9620	(002)
	22.3834	0.3109	3.9687	26.0	3.9300	(001)
150	28.5233	0.3959	3.1268	20.7	3.1200	(100)
	36.7617	0.4440	2.4428	18.9	2.4460	(101)
	46.1140	0.4100	1.9668	21.1	1.9620	(002)

Using Eq. (1) allows for directly calculating the absorption coefficient associated with the frequency corresponding to the highly absorbent region. This calculation involves using the absorption (A) and thickness (t) values to calculate the coefficient

$$\alpha = 2.303 \frac{A}{t} \tag{1}$$

The fundamental absorption edges of crystalline and amorphous materials exhibit a significant characteristic.

Understanding the transition from the valence band to the conduction band is crucial to determine a material's band gap (E_g) , which was calculated using the following equation [17]:

$$\alpha h \nu = B(h \nu - E_q)^r \tag{2}$$

The constant B in the equation varies based on material structure, optical energy gap (E_g) , and index r

The absorption of electromagnetic radiation can cause electronic transitions resulting in different r values, such as 1/2, 3/2, 2, or 3. UV-visible spectra is commonly used to determine the absorption coefficient for various wavelengths of electromagnetic radiation.

To calculate E_g , the linear plots are analyzed and extrapolated to zero absorbance [18,19].

The optical absorbance curves of Nb_2O_5 thin films prepared using a constant dc power of 50 W at different substrate temperatures (RT, 100, and 150°C) in the wavelength range of 200-800 nm is presented in Fig. (4). It can be observed that the films exhibit high absorbance in the UV region. As the substrate temperature increased, there was a decrease in absorbance, which can be attributed to the reduction of defects. This improvement in crystallinity and reduction in optical scattering at grain boundaries contributed to the reduced absorbance [20].

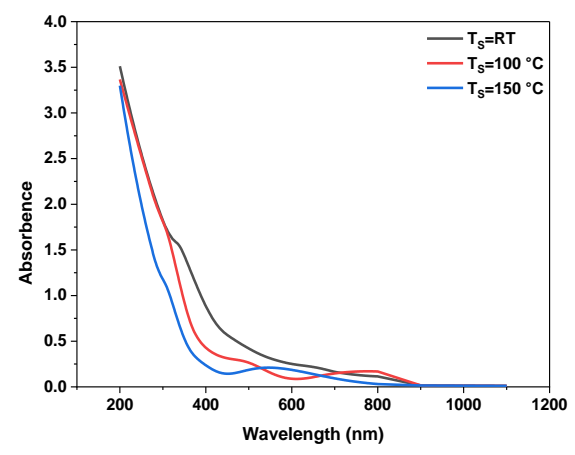


Fig. (4) UV-visible absorbance for Nb_2O_5 thin films deposited at different substrate temperatures

Figure (5) presents the Tauc's plot for Nb₂O₅ thin films deposited using a 50W dc power source at various substrate temperatures. The outcomes revealed an increase in the energy gap from 4.05 to 4.60 eV as the substrate temperature increased from room temperature to 150°C. This increase in substrate temperature corresponds to a rise in the oxygen content within the deposited thin film. As the oxygen content increases, oxygen vacancies within the film decrease. The variation in oxygen content with changing substrate temperature directly influences the energy band gap of the thin film. Specifically, an increase in oxygen content can lead to an expansion of the energy bandgap. This effect widens the energy gap between valence and conduction bands by accepting electrons from oxygen atoms [21].

Figure (6) presents 3D AFM images and cumulative particle size histograms for the surface of Nb_2O_5 thin films deposited on quartz substrates using reactive dc sputtering, maintaining a constant dc power of 50 W, while varying the substrate temperature (RT, 100° C, and 150° C).

The AFM images reveal a consistent and uniform surface texture characteristic of the Nb₂O₅ films deposited through the dc sputtering process. Notably, the average particle size experiences an increase from 34.11 to 45.56 nm as the substrate temperature is raised from RT to 150°C. Interestingly, the samples exhibit a reduction in surface roughness from 4.7 to 3.77 nm as

the substrate temperature is elevated from RT to 150°C. This phenomenon can be attributed to the higher temperature facilitating the merging of smaller attached particles on the surface, leading to an increase in particle diameters and, consequently, a reduction in surface roughness [22]. These findings align with previously reported research and underscore the critical role of surface roughness in gas-sensing applications. By optimizing the substrate temperature during the deposition process, it is possible to control the surface morphology, particle size, and roughness of the Nb₂O₅ thin films, all of which can significantly impact their performance and suitability for gassensing applications.

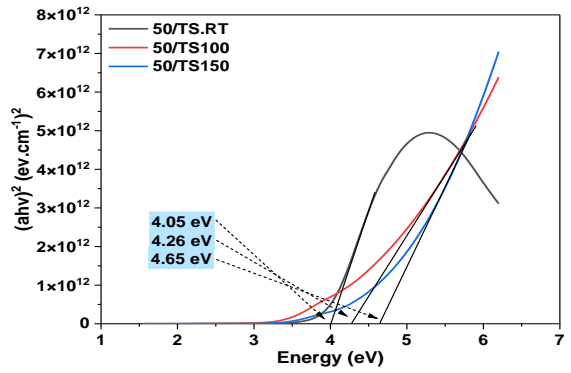


Fig. (5) Tauc's plot for Nb_2O_5 thin films deposited at different substrate temperatures

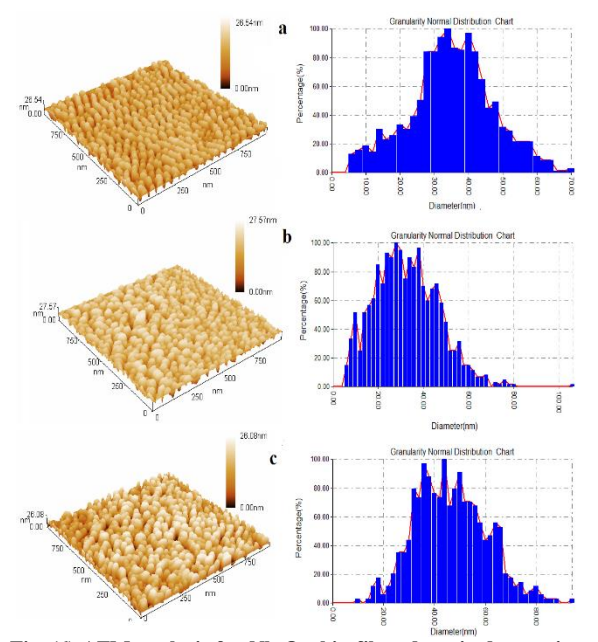


Fig. (6) AFM analysis for Nb_2O_5 thin films deposited at various substrate temperatures: (a) RT, (b) $100^{\circ}C$, and (c) $150^{\circ}C$

Table (2) lists the average diameter and average roughness from the analysis of AFM results for Nb_2O_5 thin films deposited at different substrate temperatures.

Figure (7) illustrates the EDX spectra of Nb₂O₅ thin films deposited on quartz slide substrates at various temperatures (RT, 100, and 150°C) using a constant sputtering power of 50 W. The EDX spectra exhibit

multiple peaks corresponding to the emission lines of oxygen (O) and niobium (Nb). Notably, an increase in substrate temperature leads to higher oxidation levels, resulting in an elevated oxygen concentration from 80.5 at.% to 94.2 at.% and a decrease in Nb concentration from 19.5 at.% to 5.8 at.%. This process potentially reduces the number of electron vacancies, may cause to a decline in the concentration of charge carriers [23]. Excess oxygen beyond its stoichiometric ratio on the surface of nanoparticles can be attributed to the presence of adsorbed oxygen species originating from the surrounding environment.

Table (2) AFM parameters for Nb_2O_5 thin films deposited at different substrate temperatures

Substrate Temperature (°C)	Average Diameter (nm)	Average Roughness (nm)	
RT	34.11	4.7	
100	36.35	4.27	
150	45.56	3.77	

Hall measurements determined the charge carriers, concentration (n_H) , and Hall mobility (μ_H) of Nb₂O₅ thin films deposited at various substrate temperatures. Also, all samples exhibited n-type behavior. Increasing substrate temperature leads to improved mobility of charge carriers. This improvement is attributed to enhanced crystallinity and reduced structural defects at temperatures. With fewer mechanisms obstructing their movement, charge carriers experience less resistance and, thus, greater mobility [22]. The overall charge carrier density decreases indicate on decrease the concentration of oxygen vacancies, it means that there are fewer available sites for the generation of free charge carriers, as shown in table (3). This phenomenon is significant because it directly impacts the electrical behavior of the material.

A scientific investigation was conducted to study how deposition temperature affects the sensitivity of thin films, with the goal of optimizing the operating temperature for the highest sensing performance. The experimental results illustrate the changes in resistance with operating temperature of Nb_2O_5 thin films at different substrate temperatures while exposed to NH_3 gas. The analysis involved reducing gas (NH_3) at a concentration of 31.82 ppm. The results demonstrate a clear n-type behavior, indicating a decrease in resistance when exposed to the reducing gas [24].

The variation in resistance observed by the sensor is solely influenced by the presence and quantity of specific gases of interest [25]. he sensitivity of the sensor can be assessed using Eq. (3) and the calculation method delineated in reference [26].

$$S = \left| \frac{(R_g - R_a)}{R_a} \right| \times 100\% \tag{3}$$

The operating temperature is the temperature at which the sensor's resistance reaches a steady state and remains consistent. In the given formula, S denotes the sensitivity. Conversely, R_a and R_g stand for the electrical resistance of the film when measured in the

absence and presence of gas, respectively. The study maintained a consistent NH₃ target gas concentration at 31.82 ppm in atmospheric air.

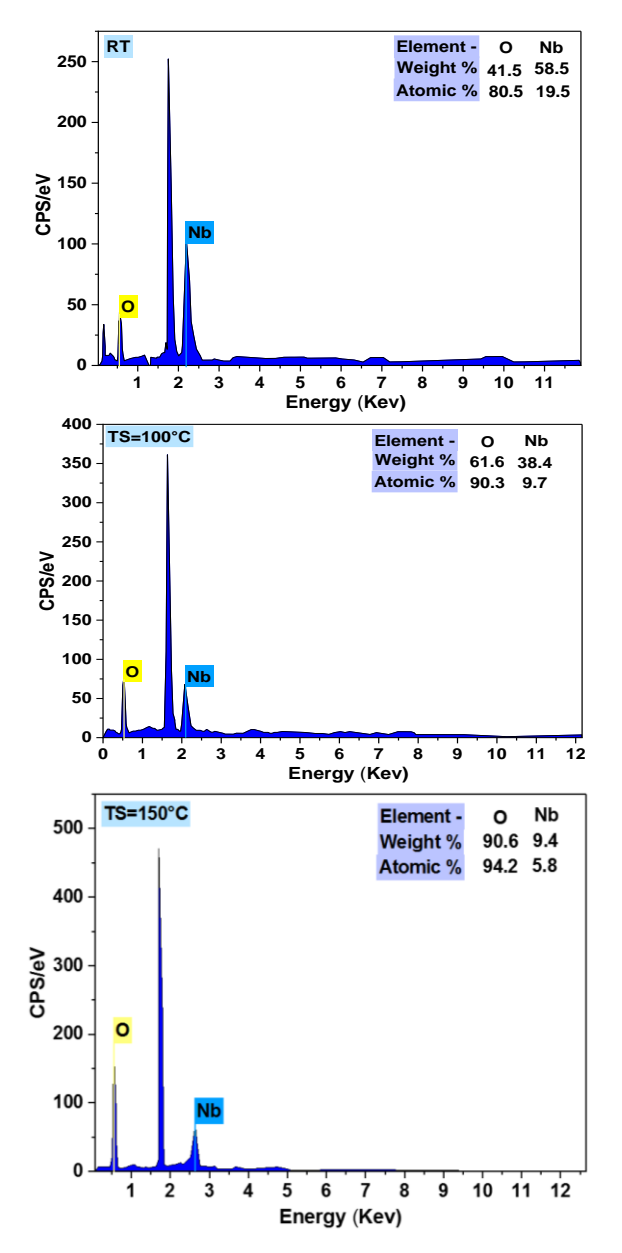


Fig. (7) EDS results for Nb_2O_5 thin films prepared at a constant power of 50 W and various substrate temperatures

Table (3) Hall effect measurements for Nb_2O_5 thin films prepared at different substrate temperatures

T _s (°C)	n×10 ¹² (cm ⁻³)	µн (cm²/V.s)	σ _{RT} (Ω ⁻¹ .cm ⁻¹)	Type
RT	7.68	107.40	1.32E-04	n-type
100	4.11	321.00	2.11E-04	n-type
150	3.23	652.00	3.37E-04	n-tvpe

Figure (8) depicts the changes in gas sensitivity among various Nb_2O_5 thin film samples. These samples were deposited using a consistent power level of 50 W but at different substrate temperatures. The measurements were taken in response to NH_3 gas as a function of operating temperature. The NH_3 gas sensor

exhibited remarkable sensitivity, reaching 33.3% when manufactured with a power setting of 50 W at room temperature (RT) and an operating temperature of 200°C.

From the results we noticed that the when the substrate temperatures increase from room temperature to 150°C led to a decline in sensitivity. One reasonable explanation for this behaviour depends on the thermodynamics of gas adsorption. As well as the temperatures increased, the kinetic energy of gas molecules increases. This increasing in the energy can overcome the adsorption energy barriers, leading to a higher rate of desorption of gas molecules from the sensor surface. In addition, the grain boundaries in the thin films can act as potential sites for gas adsorption. The number grain boundaries reduce when the substrate temperatures increase. From the results we noticed that the when the substrate temperatures increase from room temperature to 150°C led to a decline in sensitivity. One reasonable explanation for this behaviour depends on the thermodynamics of gas adsorption. As well as the temperatures increased, the kinetic energy of gas molecules increases. This increasing in the energy can overcome the adsorption energy barriers, leading to a higher rate of desorption of gas molecules from the sensor surface. In addition, the grain boundaries in the thin films can act as potential sites for gas adsorption. The number grain boundaries reduce when the substrate temperatures increase. These finding s are consistent with a prior study [26].

The response time of a gas sensor is the duration it takes for the sensor's conductance to reach 90% of its maximum or minimum value when exposed to oxidizing or reducing gases. This is expressed in Eq. (4). Recovery time, on the other hand, is the duration required for the sensor's conductance to return to a level within 10% of the initial baseline value once the gas flow stops. This is defined in Eq. (5) [27].

$$t_{response} = |\mathbf{t}_{gas(on)} - \mathbf{t}_{gas(off)}| \times 0.9$$
 (4)
$$t_{recovery} = |\mathbf{t}_{gas(off)} - \mathbf{t}_{gas(recovery)}| \times 0.9$$
 (5)

Figure (9) depicts the connection between response time and recovery time for Nb_2O_5 thin films at different operating temperatures. These films were created on a p-type Si wafer (100) using a 31.82 ppm NH₃: air mixture. The plot highlights a swift 10s response time and a 31s recovery time. This underscores the NH₃ gas sensor's capacity to swiftly react when a sufficient amount of gas is available for the chemical reaction.

Gas sensors require more time to recover than to respond because of the desorption process. When a gas sensor detects a specific gas, it causes changes in its electrical characteristics due to gas molecules adhering to the sensor's surface. However, when the gas is no longer present, the sensor needs to release or desorb these gas molecules from its surface and return to its initial state. The time required for recovery is usually longer than the response time due to the desorption process.

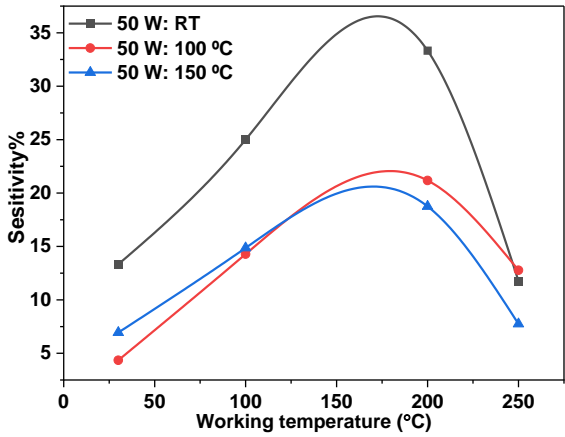
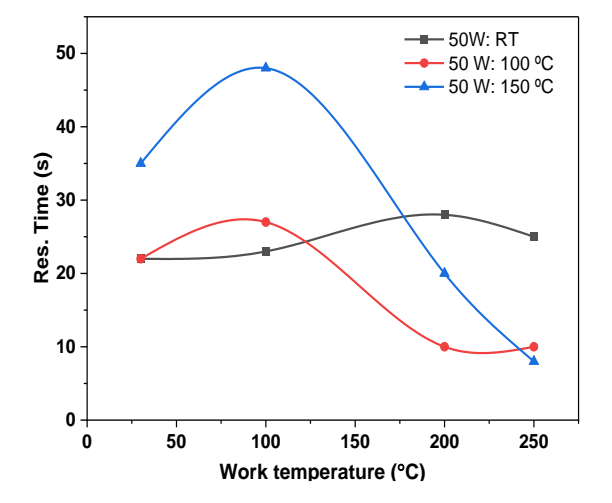


Fig. (8) NH_3 gas sensitivity vs. working temperature for Nb_2O_5 thin films prepared at different substrate temperatures

Table (4) provides data on response time, recovery time, and sensitivity percentage for NH $_3$ gas at four distinct operational temperatures (30°C, 100°C, 200°C, and 250°C) of Nb $_2$ O $_5$ thin films. These films were grown using varying substrate temperatures.

Table (4) Response time, recovery time, and sensitivity % for Nb₂O₅ thin films deposited at various substrate temperatures

Sample	Temp. (°C)	Sensitivity (%)	Response Time (s)	Recovery Time (s)
	30	13.3	22.0	35.0
50 W· RT	100	25.0	23.0	31.0
30 W. KI	200	33.3	28.0	55.0
	250	11.8	25.0	45.0
	30	4.3	22.0	50.0
50 W: 100 °C	100	14.3	27.0	45.0
50 W. 100 °C	200	21.2	10.0	50.0
	250	12.8	10.0	30.0
	30	6.9	35.0	50.0
50 W: 150 °C	30	14.9	48.0	50.0
30 W. 130 °C	100	13.3	22.0	35.0
	200	25.0	23.0	31.0



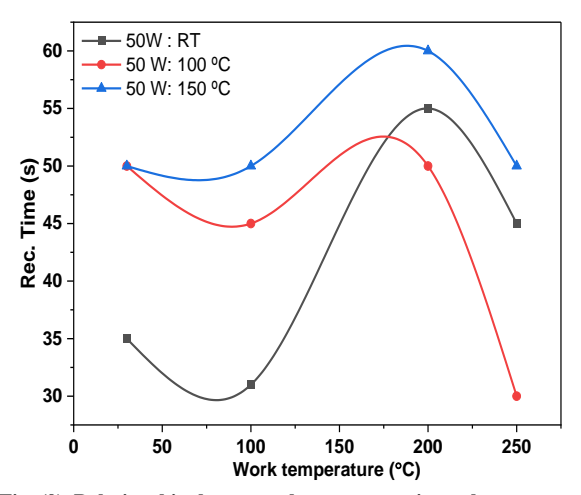


Fig. (9) Relationship between the response time, the recovery time, and the operating (working) temperature for Nb_2O_5 thin films at different substrate temperatures

4. Conclusions

In this research study, high-quality thin films of Nb₂O₅ were successfully deposited using commonly used sputtering technique. polycrystalline structure of the Nb₂O₅ thin films with a hexagonal phase. The direct optical energy gap increased with the substrate temperature, and so did the particle size of the films. The NH₃ gas sensor was tested with a power setting of 50 W at room temperature (RT) and an operating temperature of 200°C, and it showed an excellent sensitivity of 33.3% at 200°C. The sensor's response time was rapid, only 10 s when utilizing a substrate temperature of 150°C. Meanwhile, for the sample prepared with a substrate temperature of 100°C, the recovery time was the fastest at 30 s.

References

- [1] A.A. Atta et al., "Influence of argon flow rate on structural and optical properties of transparent Nb2O5 thin films", *Opt. Quantum Electron.*, 51 (2019) 1-17.
- [2] M. Mazur et al., "Determination of optical and mechanical properties of Nb₂O₅ thin films for solar cells application", *Appl. Surf. Sci.*, 301 (2014) 63-69.
- [3] R.A. Rani et al., "Nanoporous Nb₂O₅ hydrogen gas sensor", *Sens. Actuat. B Chem.*, 176 (2013) 149-156.
- [4] Ö.D. Cöcskun and S. Demirela, "The optical and structural properties of amorphous Nb₂O₅ thin films prepared by RF magnetron sputtering", *Appl. Surf. Sci.*, 277 (2013) 35-39.
- [5] B. Xiao et al., "MXenes: Reusable materials for NH3 sensor or capturer by controlling the charge injection", *Sens. Actuat. B Chem.*, 235 (2016) 103-109.
- [6] S.B. Ogale, T.V. Venkatesan and M. Blamire, "Functional metal oxides: New science and novel applications", John Wiley & Sons (2013).
- [7] R. Chandrasekharan et al., "Thermal oxidation of

- tantalum films at various oxidation states from 300 to 700 C", *J. Appl. Phys.*, 98(11) (2005) 114908.
- [8] J.-P. Masse et al., "Stability and effect of annealing on the optical properties of plasma-deposited Ta₂O₅ and Nb₂O₅ films", *Thin Solid Films*, 515(4) (2006) 1674-1682.
- [9] H. Szymanowski et al., "Optical properties and microstructure of plasma deposited Ta₂O₅ and Nb₂O₅ films", *J. Vac. Sci. Technol. A Vac. Surf. Films*, 23(2) (2005) 241-247.
- [10] S.H. Mujawar et al., "Electrochromic properties of spray-deposited niobium oxide thin films", *Solid State Ionics*, 177(37-38) (2006) 3333-3338.
- [11] K. Wasa, I. Kanno and H. Kotera, "Handbook of sputter deposition technology: fundamentals and applications for functional thin films, nano-materials and MEMS", William Andrew (2012).
- [12] M.K. Khalaf et al., "Thin film technique for preparing nano-ZnO gas sensing (O₂, NO₂) using Plasma Deposition", *Int. J. Appl. Innov. Eng. Manag*, 2 (2013) 178-184.
- [13] A. A. Atta et al., "Effect of thermal annealing on structural, optical and electrical properties of transparent Nb_2O_5 thin films", *Mater. Today Commun.*, 13 (2017) 112-118.
- [14] M.C. Morris et al., "Standard X-ray Diffraction Powder Patterns", International Centre for Diffraction data (ICDD), monograph 25, section 15 (1978) p. 43.
- [15] J.N. Nguu, "Fabrication and characterization of TiO₂/Nb₂O₅ composite photo-electrodes deposited using electrophoretic technique for application in Dye-sensitized solar cells", no. December (2017) 141.
- [16] K. Huang et al., "Nanoscale conductive niobium oxides made through low temperature phase transformation for electrocatalyst support", *RSC Adv.*, 4(19) (2014) 9701-9708.
- [17] E.A. Davis and Nf. Mott, "Conduction in noncrystalline systems V. Conductivity, optical absorption and photoconductivity in amorphous semiconductors", *Philos. Mag.*, 22(179) (1970)

- 903-922.
- [18] S. Xu and Z. L. Wang, "One-dimensional ZnO nanostructures: solution growth and functional properties", *Nano Res.*, 4 (2011) 1013-1098.
- [19] N. Usha, R. Sivakumar and C. Sanjeeviraja, "Electrochromic properties of radio frequency magnetron sputter deposited mixed Nb₂O₅: MoO₃ (95:5) thin films cycled in H⁺ and Li⁺ ions", *Mater. Sci. Semicond. Process.*, 30 (2015) 31-40.
- [20] E.T. Salim and H.T. Halboos, "Synthesis and physical properties of Ag doped niobium pentoxide thin films for Ag-Nb₂O₅/Si heterojunction device", *Mater. Res. Exp.*, 6(6) (2019) 66401.
- [21] D. Zhang et al., "Effect of substrate temperature on the microstructure, optical, and electrical properties of reactive DC magnetron sputtering vanadium oxide films", *phys. stat. sol.*, 209(11) (2012) 2229-2234.
- [22] S. Ghosh et al., "Effect of substrate temperature on the physical properties of copper nitride films by rf reactive sputtering", *Surf. Coat. Technol.*, 142 (2001) 1034-1039.
- [23] N. Usha et al., "Effect of substrate temperature on the properties of Nb₂O₅:MoO₃ (90:10) thin films prepared by rf magnetron sputtering technique", *J. Alloys Compd.*, 649 (2015) 112-121.
- [24] M. Shaban, K. Abdelkarem and A.M. El Sayed, "Structural, optical and gas sensing properties of Cu₂O/CuO mixed phase: effect of the number of coated layers and (Cr+S) co-Doping", *Phase Trans.*, 1 (2019) 1-13.
- [25] B. Karunagaran et al., "TiO₂ thin film gas sensor for monitoring ammonia", *Mater. Charact.*, 58(8-9) (2007) 680-684.
- [26] M.O. Salman, M.A. Kadhim and A.A. Khalefa, "CdO:SnO₂ Composite UV-Assisted Room Temperature Ozone Sensor", *Iraqi J. Sci.*, 64(3) (2023) 1190-1202.
- [27] N.K. Abbas, I.M. Ibrahim and M.A. Saleh, "Characteristics of MEH-PPV/Si and MEH-PPV/PS heterojunctions as NO₂ gas sensors", *Silicon*, 10 (2018) 1345-1350.